



Comparison of Hindlimb Muscle Architecture Properties in Small-Bodied, Generalist Mammals Suggests Similarity in Soft Tissue Anatomy

Mark A. Wright¹ · Karen E. Sears² · Stephanie E. Pierce¹

Accepted: 2 March 2022

© The Author(s), under exclusive licence to Springer Science+Business Media, LLC, part of Springer Nature 2022

Abstract

For the first 100+ million years of their evolutionary history, the majority of mammals were very small, and many exhibited relatively generalized locomotor ecologies. Among extant mammals, small-bodied, generalist species share similar hindlimb bone morphology and locomotor mechanics, but details of their musculature have not been investigated. To examine whether hindlimb muscle architecture properties are also similar, we dissected hindlimb muscles of the gray short-tailed opossum (*Monodelphis domestica*) and aggregated muscle properties from the literature for three other small-bodied mammals (*Mus musculus*, *Rattus norvegicus*, *Cavia porcellus*). We then studied hindlimb musculature from a whole-limb perspective and by separating the limb into nine anatomical regions. The region analysis explained substantially more variance in the data ($r^2: 0.601 > 0.074$) but only detected six statistically significant pairwise species differences in muscle architecture properties. This finding suggests either deep conservation of therian hindlimb muscle properties or, more likely, a biomechanical constraint imposed by small body size. In addition, we find specialization for either large force production (i.e., PCSA) or longer active working ranges (i.e. long muscle fascicles) in proximal limb regions but neither specialization in more distal limb regions. This functional pattern may be key for small mammals to traverse across uneven and shifting substrates, regardless of environment. These findings are particularly relevant for researchers seeking to reconstruct and model soft tissue properties of extinct mammals during the early evolutionary history of the clade.

Keywords Muscle architecture · Hindlimb · Body size · Mammal · Terrestrial · Quadrupedal

Introduction

Body size influences almost every aspect of an animal's biology, including both ecological (e.g., diet, habitat, geography) and physiological (e.g., metabolism, body temperature, life span) traits (Wilson and Mittermeier 2009, 2011; Nowak 2018). Modern mammals exemplify the influence of body size with masses that range from the 2 g insectivorous

Etruscan shrew to the massive 190,000 kg filter-feeding blue whale (Polly 2007; Jones et al. 2009; McClain et al. 2015). This vast body size range contrasts with the early evolutionary history of the mammalian lineage (Fig. 1a): throughout the Mesozoic, mammals were no larger than 10 kg and, in most cases, were orders of magnitude smaller (Slater 2013). The limited range of masses throughout the Mesozoic is suggested to be a constraint due to competitive displacement and/or predation from dinosaurs and other larger terrestrial fauna (Kielan-Jaworowska et al. 2004; Kemp 2005; Brocklehurst et al. 2021), which is supported by the rapid increase in body size immediately following the K-Pg mass extinction (Slater 2013; Lyson et al. 2019). While Mesozoic mammals were capable of evolving highly specialized ecological adaptations, as demonstrated by recent fossil discoveries of swimming (Ji et al. 2006), digging (Luo and Wible 2005), and gliding (Meng et al. 2006) forms, the vast majority of known mammal species from Mesozoic ecosystems exhibited more generalist locomotor ecologies (Luo 2007; Panciroli et al. 2021).

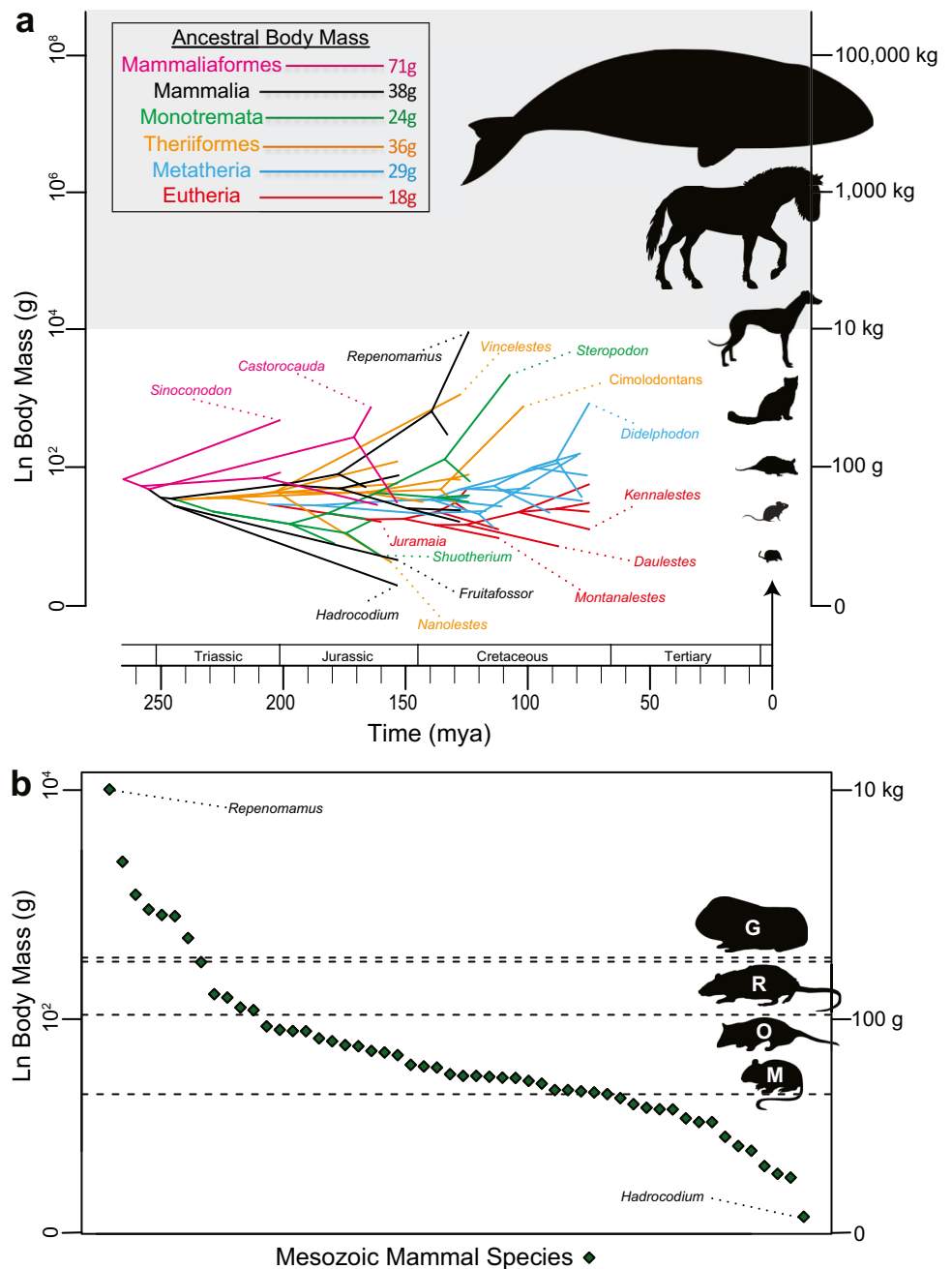
✉ Mark A. Wright
markwright@g.harvard.edu

✉ Stephanie E. Pierce
spierce@oeb.harvard.edu

¹ Museum of Comparative Zoology and Department of Organismic and Evolutionary Biology, Harvard University, Cambridge, MA, USA

² Departments of Ecology and Evolutionary Biology and Molecular, Cell, and Developmental Biology, University of California at Los Angeles, Los Angeles, CA, USA

Fig. 1 a Ancestral state reconstruction of body mass in Mesozoic mammals using the dataset of Slater (2013) and the ‘phytools’ package in R (Revell 2012). The value for cimolodontans is a species average for the clade. Left Y-axis is natural log-scaled body mass, while right Y-axis is non-logged body mass. Greyed-out area denotes body masses larger than any known Mesozoic mammal fossil found to date. **b** Range of estimated body masses of 54 Mesozoic mammal species (green diamonds, in decreasing size order) from the dataset of Slater (2013). Body masses of the four species studied here (G: guinea pig; M: mouse; O: opossum; R: rat) are represented by horizontal dashed lines. All silhouettes are from phylopic.org



Among extant small-bodied mammals, ecomorphological analyses have shown that highly specialized species (e.g., swimmers, diggers, and gliders) are readily distinguished by limb bone morphology; in contrast, species with terrestrial, scansorial, and non-specialized arboreal habits are far more similar, showing relatively minor morphological variation within the broader context of small mammal ecological diversity (Sargis 2002; Álvarez et al. 2013; Chen and Wilson 2015; Weaver and Grossnickle 2020). Recent studies have also demonstrated that stylopod (humerus or femur) bone morphology and internal microstructure are largely similar among rodents and mustelids of varying locomotor ecology

(Amson and Kilbourne 2019; Hedrick et al. 2020; Kilbourne 2021); in both cases, only fossorial species had distinctly specialized bones, suggesting that proximal limb elements may be more similar than distal limb elements. Many small-bodied terrestrial, scansorial, and non-specialized arboreal mammals further tend to utilize “crouched” limb postures during locomotion (Jenkins 1971; Riskin et al. 2016) with plantigrade feet (Kubo et al. 2019), although still exhibiting variation in footfall patterns and center-of-mass mechanics (Biknevicius et al. 2013). Small-bodied mammals that utilize crouched postures favor energy saving mechanisms such as increased stride frequency compared to larger more upright

mammals and, consequently, running is relatively cheaper in terms of locomotor cost than walking (Reilly et al. 2007; Bishop et al. 2008; Riskin et al. 2016). Therefore, in spite of remarkable ecological and phylogenetic breadth, many mammals of small sizes share similar skeletal patterns and posture, reflecting that body size is capable of greatly influencing anatomy.

While the link between limb bone morphology, posture, and ecology has been investigated among small-bodied mammals, much less is known about muscles, the actuators of movement. Architectural properties of muscles such as fascicle length and physiological cross-sectional area (PCSA) are proxies for the contraction velocity and force production capabilities of a muscle, respectively (Lieber 2002). Some muscles also have pennate fibers that are arranged at an angle to the central tendon, allowing gearing to vary with load so that low-load contractions favor velocity and high-load contractions favor force output (Azizi et al. 2008). Although limb muscle architecture of small-bodied mammals has been studied independently for the mouse (Charles et al. 2016), rat (Eng et al. 2008), and guinea pig (Powell et al. 1984), whether there are overarching patterns across small taxa has not been investigated.

Here, we aimed to quantitatively assess hindlimb muscle architecture across small-bodied, generalist mammals and test whether architecture shows a similar pattern to bone morphology and posture. Generalist species are those that are primarily terrestrial but regularly engage in behaviors associated with other ecological groups (e.g., swimming, digging, climbing; see Panciroli et al. 2021 for further discussion on “generalist” species). We hypothesized that, based on broad-scale similarities in bone anatomy and limb posture, generalist small-bodied mammals will also exhibit similar patterns of muscle anatomy. Considering many Mesozoic mammals were generalists, this question has important implications for the early evolutionary history of mammals. First, we provide new data on the hindlimb muscle topology and architecture of the gray short-tailed opossum, *Monodelphis domestica*, a small marsupial often suggested to be an extant model of plesiomorphic therian hindlimb anatomy (Argot 2001; Parchman et al. 2003; Lammers et al. 2006; Ferner et al. 2009; Shapiro et al. 2014; Diogo et al. 2016; Urban et al. 2017; Diogo et al. 2018). Then, we compare hindlimb muscle architecture properties from the whole limb and across different anatomical regions in four species that engage in terrestrial-scansorial behaviors (opossum, mouse, rat, guinea pig), and span an order of magnitude in body mass that encompasses much of the estimated body mass range of Mesozoic mammals (Fig. 1b). Overall, we find that hindlimb muscle architecture properties among these species is largely indistinguishable. The findings of this study can help inform our understanding of musculoskeletal anatomy in mammals and provide insight

for future soft tissue reconstructions during the early evolutionary history of the clade.

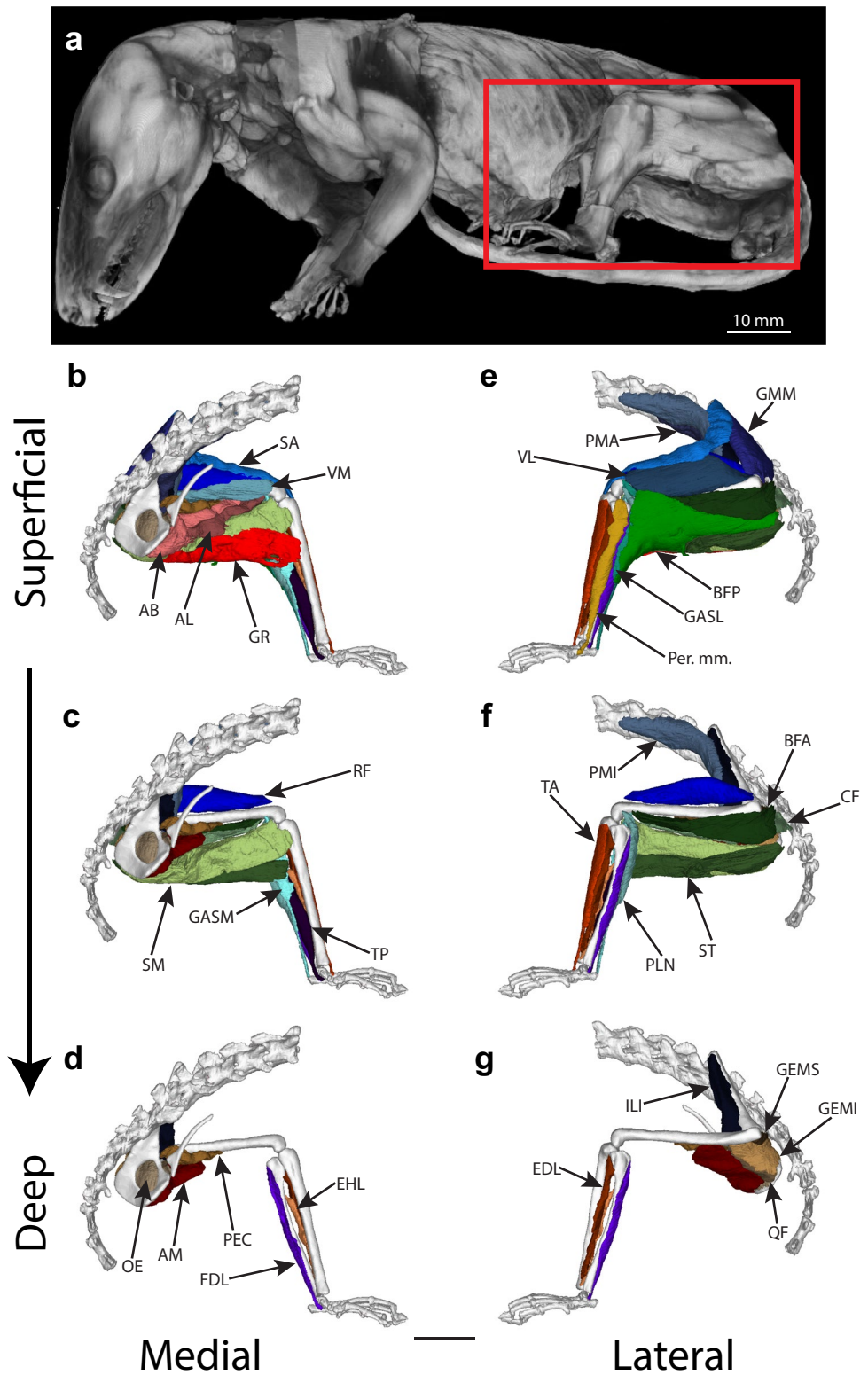
Materials and Methods

Monodelphis Hindlimb Muscle Anatomy

A combination of contrast-stained microcomputed tomography (μ CT) scans and physical muscle dissections were used to determine hindlimb muscle topology (origins, insertions) and internal architecture for the gray short-tailed opossum (*Monodelphis domestica*). To determine muscle origins and insertions, one cadaveric specimen was thawed, skinned, gutted, and fixed for 24 h in 10% neutral-buffered formalin solution. Following fixation, the specimen was immersed in a 2.5% solution of phosphomolybdic acid (PMA) to enhance soft tissue contrast (Pauwels et al. 2013). To ensure full penetration of muscle tissue, the specimen was agitated regularly and scanned after 3 weeks, 5 weeks, and 8 weeks using a Bruker Skyscan 1173 (voxel size: 35.71 μ m³) and with the following settings: 139 kV, 71 μ A, and a 1.0 mm aluminum filter. Tomograms from the 8-week scan were reconstructed as a TIFF image stack using Skyscan NRecon software and imported into Mimics v19 (Materialise, Leuven, Belgium) for segmentation of the left hindlimb. All muscles that crossed the hip, knee, and ankle joints were segmented and identified using existing literature on opossum anatomy and vertebrate muscle homologies (Stein 1981; Diogo et al. 2018) and later confirmed during dissection (Figs. 2 and 3). Four muscles (mm. peroneus longus, peroneus brevis, peroneus tertius, and peroneus digiti quinti) were not readily differentiated in the stained specimen and were subsequently visualized as one bundle of “peroneus” muscles in the reconstructed three-dimensional (3D) model. However, their presence as four distinct muscles was confirmed during dissection. Muscle attachment sites were recorded for each muscle based on the 3D meshes generated from the segmented bones and muscles, and these sites were also confirmed during dissection (Table 1). To aid in visualization and comparison, these attachments were then digitally painted onto 3D bone meshes using Autodesk Mudbox (Fahn-Lai et al. 2020; Regnault et al. 2020).

Both the right and left hindlimbs from two additional cadaveric specimens (body mass = 110.28 g and, 114.08 g) were dissected to collect architectural properties for each muscle following standard protocols (Eng et al. 2008; Charles et al. 2016; Cuff et al. 2016; Fahn-Lai et al. 2020; Regnault et al. 2020). Specimens were thawed, skinned, and gutted, and then transected through the lumbar region to isolate the hindlimbs (and the anterior part of the body was refrozen for future use). The hindlimbs were then fixed in a pose where each joint was flexed at 90° with the limbs abducted at 45° from the midline of the body and fixed in 10% neutral-

Fig. 2 **a** Micro-CT scan of contrast-stained *Monodelphis domestica* specimen with the hindlimb outlined in red. **b-g** Segmented hindlimb muscles of *Monodelphis* arranged from superficial (top) to deep (bottom) and medial (left) to lateral (right). See Table 1 for muscle abbreviations. (“Per. mm.” refers to all four peroneus muscles, which were separated by fascia too thin to be segmented individually). Scale bar equals 10 mm



buffered formalin solution for 24–48 h. The limbs were dissected under a magnifier lamp. Muscles were identified, removed, rinsed in saline to remove excess fixative, and blotted dry.

Four architecture properties were recorded for each muscle: muscle mass (MM, in g), muscle length (ML, in mm), pennation angle (PA, in degrees), and fascicle length (FL, in mm). Previous

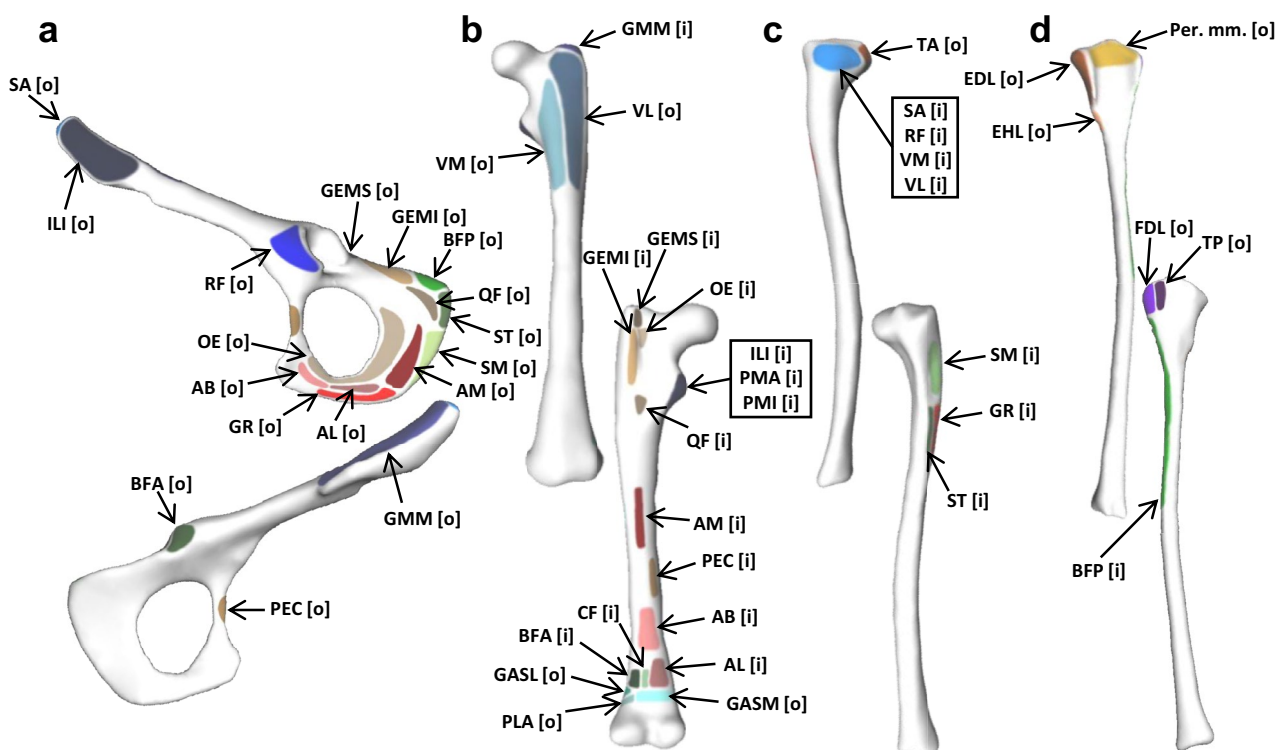


Fig. 3 Muscle attachments in the hindlimb of *Monodelphis domestica* depicted on: **a** left pelvis in lateral (above) and medial (below) views; **b** left femur in dorsal (above) and ventral (below) views; **c** left tibia in dorsal (above) and ventral (below) views; **d** left fibula in dorsal (above) and ventral (below) views. Muscle attachments on the verte-

brae (origins of PMA, PMI, and CF) and pes (insertions of all muscles in the four “leg” regions) are not included. Muscle origins are denoted by [o] and insertions by [i]. See Table 1 for muscle abbreviations

work has demonstrated that muscle fibers arranged in series can be activated simultaneously and function as a single muscle fiber (Bodine et al. 1982), and we follow Charles et al. (2016) in assuming functional similarity between fascicle and fiber length. Tendon mass (TM, in g) and length (TL, in mm) were also recorded for each muscle, where possible, but these data were not used in subsequent analyses. Masses were recorded on an Intelligent-Lab Precisa XC 220A scale, while linear and angular measures were recorded from digital photographs using ImageJ software (Rasband 1997-2018). From these measurements, physiological cross-sectional area (PCSA, mm²) was calculated using the following equation:

$$PCSA = \frac{(MM)(\cos PA)}{(FL)(\rho)}$$

where ρ is the density of mammal skeletal muscle, taken as 0.001056 g/mm⁻³ (Ward and Lieber 2005). The mean (\pm standard deviation) hindlimb muscle architecture data for *M. domestica* are provided in Table 2, and the raw data are provided in Online Resource 1.

Muscle Homologies and Properties in this Dataset

In addition to the opossum, we compiled hindlimb muscle data from the literature for three other small-bodied, generalist mammals with a range of body masses: the house mouse *Mus musculus* (23 g) (Charles et al. 2016), the brown rat *Rattus norvegicus* (323 g) (Eng et al. 2008), and the guinea pig *Cavia porcellus* (350 g) (Powell et al. 1984). For each of these species, we recorded the same five standard architecture properties for each of their hindlimb muscles as described for *Monodelphis* (Online Resource 1). To facilitate comparisons among species, four of the five muscle architecture variables (excluding PA) were scaled to body mass (BM) assuming isometric scaling (i.e., lengths \propto BM^{1/3}, areas \propto BM^{2/3}, and masses \propto BM¹) and log-normalized to reduce skew. PA is a unitless dimension and therefore is not expected to scale proportional to body mass, at least across the small size range considered here (Dick and Clemente 2016). Further, no data transformations increased the normality of PA distribution, so non-parametric analyses were used here forward.

To compare muscle architectural properties between small-bodied mammals, we first needed to determine

Table 1 The muscles of the hindlimb of the gray short-tailed opossum, *Monodelphis domestica*, identified through dissection and contrast-stained micro-CT scanning. Origins and insertions are listed for

each muscle, as well as the joint(s) that the muscle crosses and the anatomical region assigned for statistical comparisons

Muscle	Origin	Insertion	Joint(s)	Limb Region
Adductor brevis (AB)	Body of pubis	Distal ventral femur	Hip	Medial Thigh
Adductor longus (AL)	Descending ramus of pubis	Distal ventral femur	Hip	Medial Thigh
Adductor magnus (AM)	Pubo-ischial ramus	Middle ventral femur	Hip	Medial Thigh
Biceps femoris anterior (BFA)	Dorsal margin of acetabulum	Distal ventral femur	Hip	Posterior Thigh
Biceps femoris posterior (BFP)	Ischial tuberosity	Lateral proximal fibula	Hip, Knee	Posterior Thigh
Caudofemoralis (CF)	Vertebral column	Distal ventral femur	Hip	Posterior Thigh
Extensor digitorum longus (EDL)	Proximal medial tibia	Digits 2–5	Ankle	Anterior Leg
Extensor hallucis longus (EHL)	Proximal medial tibia	Digit 1	Ankle	Anterior Leg
Flexor digitorum longus (FDL)	Proximal ventral tibia	Digits 2–5	Ankle	Posterior Deep Leg
Gastrocnemius lateralis (GASL)	Lateral femoral condyle	Calcaneal tendon	Knee, Ankle	Posterior Superficial Leg
Gastrocnemius medialis (GASM)	Medial femoral condyle	Calcaneal tendon	Knee, Ankle	Posterior Superficial Leg
Gemellus superior (GEMS)	Posterior margin of acetabulum	Intertrochanteric crest	Hip	Proximal Hip
Gemellus inferior (GEMI)	Dorsal margin of ischium	Intertrochanteric crest	Hip	Proximal Hip
Gluteal muscles (GMM)	Cranial ilium above the lateral margin	Greater trochanter	Hip	Trunk
Gracilis (GR)	Ventral aspect of pubo-ischial ramus	Medial middle tibia	Hip, Knee	Medial Thigh
Iliacus (ILI)	Cranial ilium below the lateral margin	Lesser trochanter	Hip	Trunk
Obturator externus (OE)	Lateral bony margin of obturator foramen	Intertrochanteric crest	Hip	Proximal Hip
Pectineus (PEC)	Ascending ramus of pubis	Medial middle femur	Hip	Proximal Hip
Peroneus brevis (PB)	Proximal dorsal fibula	5th metatarsal	Ankle	Lateral Leg
Peroneus digiti quinti (PD5)	Proximal dorsal fibula	Digit 5	Ankle	Lateral Leg
Peroneus longus (PL)	Proximal dorsal fibula	Medial cuneiform	Ankle	Lateral Leg
Peroneus tertius (PT)	Proximal dorsal fibula	Cuboid	Ankle	Lateral Leg
Plantaris (PLN)	Lateral femoral condyle	Calcaneal tendon	Knee, Ankle	Posterior Superficial Leg
Psoas major (PMA)	Vertebral column	Lesser trochanter	Hip	Trunk
Psoas minor (PMI)	Vertebral column	Lesser trochanter	Hip	Trunk
Quadratus femoris (QF)	Body of ischium	Proximal ventral femur	Hip	Proximal Hip
Rectus femoris (RF)	Cranial margin of acetabulum	Patellar tendon	Hip, Knee	Anterior Thigh
Sartorius (SA)	Cranial aspect of ilium	Patellar tendon	Hip, Knee	Anterior Thigh
Semimembranosus (SM)	Ischium	Medial proximal tibia	Hip, Knee	Posterior Thigh
Semitendinosus (ST)	Ischial tuberosity	Medial middle tibia	Hip, Knee	Posterior Thigh
Tibialis anterior (TA)	Proximal lateral tibia	1st metatarsal	Ankle	Anterior Leg
Tibialis posterior (TP)	Proximal ventral tibia	1st metatarsal	Ankle	Posterior Deep Leg
Vastus lateralis (VL)	Lateral aspect of proximal femur	Patellar tendon	Knee	Anterior Thigh
Vastus medialis (VM)	Medial aspect of proximal femur	Patellar tendon	Knee	Anterior Thigh

muscle homologies (Online Resource 2). Not every muscle in our dataset had homologues across all four species, either because a muscle was not identified and recorded in the source study or due to ancestral muscles being lost or dividing into multiple muscle bellies during the evolution of specific lineages (Online Resource 2, Table S1). For example, marsupials lack *m. vastus intermedius*, so this muscle in the three placental species has no direct homologue for comparison in the opossum (Diogo et al. 2016). We accounted for these cases by combining measurements for muscles with multiple divisions into one value. When

combining architecture measurements for muscles with multiple divisions, we took a functionally conservative approach to ensure we did not underestimate any potentially notable variation. Muscle masses are represented by the arithmetic sum, muscle lengths are represented by the longest recorded length, pennation angles are represented by the largest recorded angles, and fascicle lengths are represented by the longest recorded length. Where muscle properties were combined in this manner, PCSA was recalculated to ensure internal consistency in the dataset (see Online Resource 2 for a full description and justification

Table 2 Muscle architecture properties for all muscles in the hindlimb of the gray short-tailed opossum, *Monodelphis domestica*. Values listed are mean \pm standard deviation for each architecture property, respectively, based on dissections of four hindlimbs (left and right from two individuals; body mass = 112.18 \pm 2.68 g). Raw data are provided in Online Resource 1

Muscle	MM (g)	ML (mm)	PA (°)	FL (mm)	PCSA (mm ²)
Adductor brevis (AB)	0.17 \pm 0.044	25.973 \pm 1.428	13.567 \pm 6.784	22.473 \pm 1.688	7.202 \pm 6.784
Adductor longus (AL)	0.058 \pm 0.017	26.658 \pm 2.143	0 \pm 0	24.527 \pm 1.412	2.268 \pm 0
Adductor magnus (AM)	0.067 \pm 0.017	18.734 \pm 1	0 \pm 0	17.032 \pm 0.827	3.721 \pm 0
Biceps femoris anterior (BFA)	0.23 \pm 0.04	34.267 \pm 3.548	16.769 \pm 8.385	28.779 \pm 2.524	7.526 \pm 8.385
Biceps femoris posterior (BFP)	0.3 \pm 0.023	27.228 \pm 1.017	14.503 \pm 2.152	20.476 \pm 1.207	13.465 \pm 2.152
Caudofemoralis (CF)	0.04 \pm 0.021	28.441 \pm 2.655	0 \pm 0	24.836 \pm 1.025	1.532 \pm 0
Extensor digitorum longus (EDL)	0.025 \pm 0.007	18.835 \pm 2.125	9.653 \pm 4.827	17.029 \pm 6.132	1.495 \pm 4.827
Extensor hallucis longus (EHL)	0.011 \pm 0.003	14.106 \pm 0.981	12.127 \pm 6.064	13.047 \pm 0.615	0.773 \pm 6.064
Flexor digitorum longus (FDL)	0.113 \pm 0.038	23.74 \pm 1.717	9.868 \pm 4.934	20.387 \pm 3.921	5.074 \pm 4.934
Gastrocnemius lateralis (GASL)	0.108 \pm 0.005	18.13 \pm 1.459	12.749 \pm 3.085	13.341 \pm 2.27	7.652 \pm 3.085
Gastrocnemius medialis (GASM)	0.053 \pm 0.011	14.565 \pm 1.627	18.611 \pm 9.306	10.992 \pm 1.866	4.563 \pm 9.306
Gemellus superior (GEMS)	0.015 \pm 0.008	7.987 \pm 1.552	0 \pm 0	6.197 \pm 1.219	2.12 \pm 0
Gemellus inferior (GEMI)	0.052 \pm 0.008	9.889 \pm 1.744	0 \pm 0	8.281 \pm 1.442	6.001 \pm 0
Gluteal muscles (GMM)	0.411 \pm 0.062	21.154 \pm 1.927	18.572 \pm 2.227	11.425 \pm 1.896	32.361 \pm 2.227
Gracilis (GR)	0.168 \pm 0.028	28.949 \pm 2.233	0 \pm 0	26.144 \pm 3.167	6.121 \pm 0
Iliacus (ILI)	0.12 \pm 0.031	20.877 \pm 2.667	12.475 \pm 7.053	17.189 \pm 1.004	6.464 \pm 7.053
Obturator externus (OE)	0.085 \pm 0.006	9.589 \pm 0.966	0 \pm 0	9.135 \pm 0.603	8.788 \pm 0
Pectineus (PEC)	0.042 \pm 0.014	14.18 \pm 4.853	0 \pm 0	10.612 \pm 1.989	3.734 \pm 0
Peroneus brevis (PB)	0.024 \pm 0.004	15.495 \pm 3.239	11.049 \pm 6.835	12.746 \pm 2.387	1.754 \pm 6.835
Peroneus digiti quinti (PD5)	0.009 \pm 0.006	15.081 \pm 2.531	0 \pm 0	10.773 \pm 2.853	0.714 \pm 0
Peroneus longus (PL)	0.04 \pm 0.01	15.98 \pm 6.483	13.319 \pm 8.64	12.148 \pm 3.754	3.101 \pm 8.64
Peroneus tertius (PT)	0.01 \pm 0.005	12.641 \pm 3.209	0 \pm 0	11.816 \pm 4.52	0.773 \pm 0
Plantaris (PLN)	0.031 \pm 0.005	18.355 \pm 1.169	12.042 \pm 6.207	14.971 \pm 4.212	2.003 \pm 6.207
Psoas major (PMA)	0.157 \pm 0.032	24.298 \pm 3.093	17.304 \pm 10.569	16.727 \pm 5.603	9.091 \pm 10.569
Psoas minor (PMI)	0.104 \pm 0.059	21.002 \pm 4.469	14.129 \pm 7.065	14.741 \pm 2.574	6.657 \pm 7.065
Quadratus femoris (QF)	0.024 \pm 0.018	9.682 \pm 3.148	0 \pm 0	7.777 \pm 2.714	2.674 \pm 0
Rectus femoris (RF)	0.25 \pm 0.015	24.3 \pm 1.235	19.424 \pm 2.924	17.165 \pm 2.127	13.095 \pm 2.924
Sartorius (SA)	0.178 \pm 0.011	25.602 \pm 2.154	12.796 \pm 6.398	22.725 \pm 2.862	7.418 \pm 6.398
Semimembranosus (SM)	0.515 \pm 0.048	30.598 \pm 0.311	17.573 \pm 3.527	24.542 \pm 0.987	18.906 \pm 3.527
Semitendinosus (ST)	0.281 \pm 0.025	29.257 \pm 2.117	18.78 \pm 9.39	24.161 \pm 2.24	10.963 \pm 9.39
Tibialis anterior (TA)	0.091 \pm 0.023	16.915 \pm 0.419	19.111 \pm 11.771	15.452 \pm 2.737	5.374 \pm 11.771
Tibialis posterior (TP)	0.058 \pm 0.013	16.746 \pm 1.221	8.349 \pm 5.358	15.243 \pm 3.307	3.641 \pm 5.358
Vastus lateralis (VL)	0.331 \pm 0.016	24.752 \pm 1.297	18.588 \pm 1.445	12.445 \pm 1.909	24.351 \pm 1.445
Vastus medialis (VM)	0.129 \pm 0.03	21.476 \pm 1.186	13.491 \pm 6.746	16.112 \pm 1.608	7.686 \pm 6.746

for assigning homology for each individual muscle). Ultimately, our processed data included 118 muscles across four species with five architecture properties reported for each muscle (Online Resource 1).

Comparison among Small-Bodied Mammals

To test whether there were any differences in whole-hindlimb muscle architecture among species, we first performed a principal coordinate analysis (PCO) on the entire dataset using the ‘regions’ package (Jones et al. 2018) in R (R Core Team 2021); PCO is a distance-based ordination

that allows for missing data in the distance matrix. We then performed a non-parametric multivariate analysis of variance (MANOVA) on the PCO axes that individually explained at least 3% of the variance (5 axes) in the dataset with species as the grouping factor. This MANOVA was performed using the ‘RRPP’ package (Collyer and Adams 2018) in R. We then sought to identify, for each muscle architecture property, which species, if any, differed in regard to that property. This step was achieved by performing five univariate analyses of variance (ANOVAs) for each architectural property individually (MM, ML, PA, FL, and PCSA) with species as the grouping factor, as well

as posthoc pairwise comparisons between species, including adjusted alpha values following the Bonferroni method for correcting for multiple comparisons (Bonferroni 1936).

We also analyzed the hindlimb in localized anatomical regions and tested whether species effects on muscle architecture variation were present in specific compartments of the hindlimb. We identified nine hindlimb regions: trunk (TR), proximal hip (PH), anterior thigh (AT), medial thigh (MT), posterior thigh (PT), anterior leg (AL), posterior superficial leg (PSL), posterior deep leg (PDL), and lateral leg (LL). To perform our region analysis, we first generated a new PCO for these data using the ‘regions’ package in R, excluding the TR and PH as these regions were almost entirely represented by the mouse and opossum (Online Resource 2, Table S1). We then performed a non-parametric MANOVA using the ‘RRPP’ package in R on the PCO axes that explained at least 3% of the variance (6 axes), but this time we included both species and muscle region as grouping factors in our model, as well as the interaction term between species and region. While this approach informs whether there is variation among regions throughout the hindlimb, it does not identify which individual regions contain variation among species. To further investigate muscle architecture variation for each region independently, we generated another set of PCOs for each region and performed non-parametric MANOVAs on the significant PCO axes (> 3%) with species as the grouping factor. For each of the muscle regions where species was a significant factor in explaining variance in muscle architecture, we performed individual univariate ANOVAs for each muscle architecture property (MM, ML, PA, FL, and PCSA), including posthoc pairwise comparisons adjusting for multiple comparisons using the Bonferroni method.

Finally, to consider the functional design of the small-bodied mammal hindlimb, we plotted two architecture variables commonly used to estimate muscle function: normalized PCSA as a proxy for force production against normalized FL as a proxy for active working range. This functional morphospace facilitates visualization of physiological trade-offs within and between muscles (Lieber 2002; Dickson and Pierce 2018). We included only the 17 homologous muscles that were identified across all four species, and convex hulls were generated around each muscle region.

Data Structure and Phylogenetic Correction

For each of our analyses, the data matrix was constructed with each row as one muscle and species as a grouping factor, as opposed to calculating weighted means for each species (Online Resource 1). This approach allowed us to account for every muscle identified for each species in the dataset, but it creates a covariance matrix that is equivalent to one with large polytomies – an issue that has not yet been

resolved for applying phylogenetic corrections to account for shared evolutionary histories (M. Collyer pers. com.). In studies that account for phylogeny, species are usually represented by one value, and multiple species are often grouped together using, for example, a behavioral or ecological category such as locomotor mode (Álvarez et al. 2013; Cuff et al. 2016; Hedrick et al. 2020). However, in our case, species is directly the grouping factor for muscles, and every muscle for each species is located at the same exact position on the phylogeny. Given that accounting for phylogeny typically removes significant differences detected or has no effect, we would anticipate that any phylogenetic corrections applied to our data would either have no effect or decrease the number of significant differences detected (Freckleton et al. 2002; Carvalho et al. 2006).

All data generated or analyzed during this study are included in this published article (and its supplementary information files).

Results

Monodelphis Hindlimb Myology and Architecture

We identified 34 hindlimb muscles in *Monodelphis domestica* (Figs. 2 and 3) that crossed the hip, knee, and ankle joints (Table 1; includes muscle abbreviations). Of the 34 muscles, 14 crossed solely the hip joint, six crossed both the hip and the knee joints, two crossed solely the knee joint, three crossed both the knee and ankle joints, and nine crossed solely the ankle joint.

Muscle architecture in the hindlimb of *M. domestica* varied depending on the location of the muscle (Table 2). Proximal hindlimb muscles that crossed the hip and inserted on the proximal femur (e.g. PEC, GEMS, GEMI, QF, and OE) were typically parallel-fibered and, had lower muscle mass (MM) and shorter fiber lengths (FL). The gluteal muscles (GMM), in contrast, instead had fairly long FL and a larger physiological cross-sectional area (PCSA). Thigh muscles that have insertions on the distal femur, proximal tibia, and proximal fibula (e.g. BFP, SM, and GR) had larger MM and pennation angles (PA) with long muscles (ML) and FL, as well as larger PCSA. The distal leg muscles, with insertions on the tarsus and pes (e.g. GASL, TA, and TP), had relatively smaller MM and smaller PCSA.

Hindlimb Muscle Variation among Small-Bodied Mammals

In the ‘whole-hindlimb’ analysis (Fig. 4), species was determined to be a significant factor influencing muscle anatomy but explained only a very small amount of the variance in the data ($p=0.004$, $r^2=0.074$). Univariate ANOVAs with posthoc

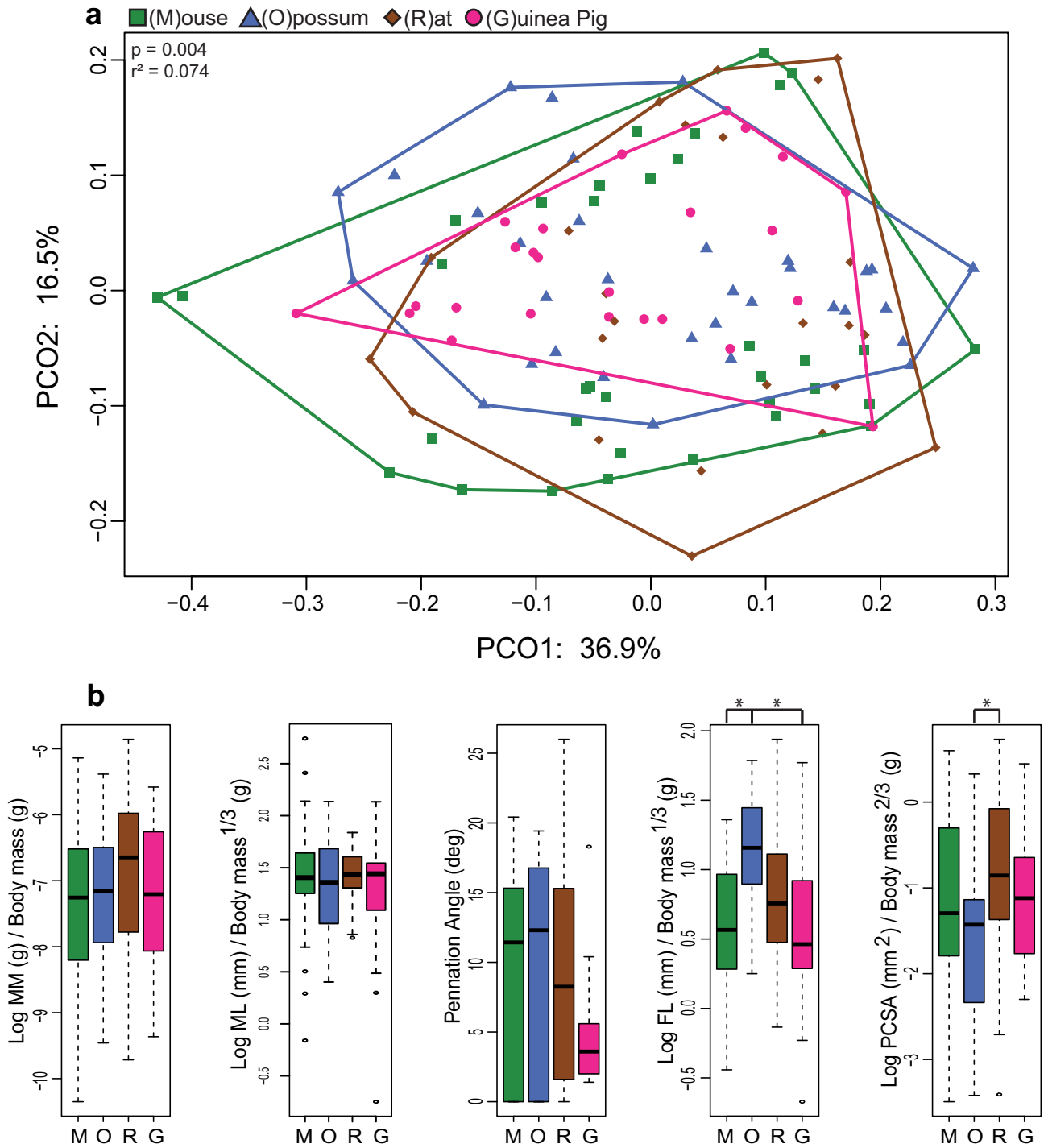


Fig. 4 **a** Principal coordinate analysis (PCO) of whole-hindlimb muscle properties and result of non-parametric MANOVA with muscles grouped by species (indicated by color). **b** ANOVA results for each individual muscle architecture property in the whole-hindlimb for

each species (also see Online Resource 2, Table S2). Significant pairwise species differences are indicated above each bar plot by an asterisk

pairwise species comparisons identified only three significant differences in muscle architecture: the opossum had longer FLs than either the mouse or guinea pig and smaller PCSAs than the rat (Online Resource 2, Table S2). The ‘regional’

analysis (Fig. 5a) explained substantially more of the variance in the data ($r^2=0.601$); both species ($p<0.001$) and region ($p<0.001$) were significant, while the interaction between species and region was not significant ($p=0.093$). Posthoc

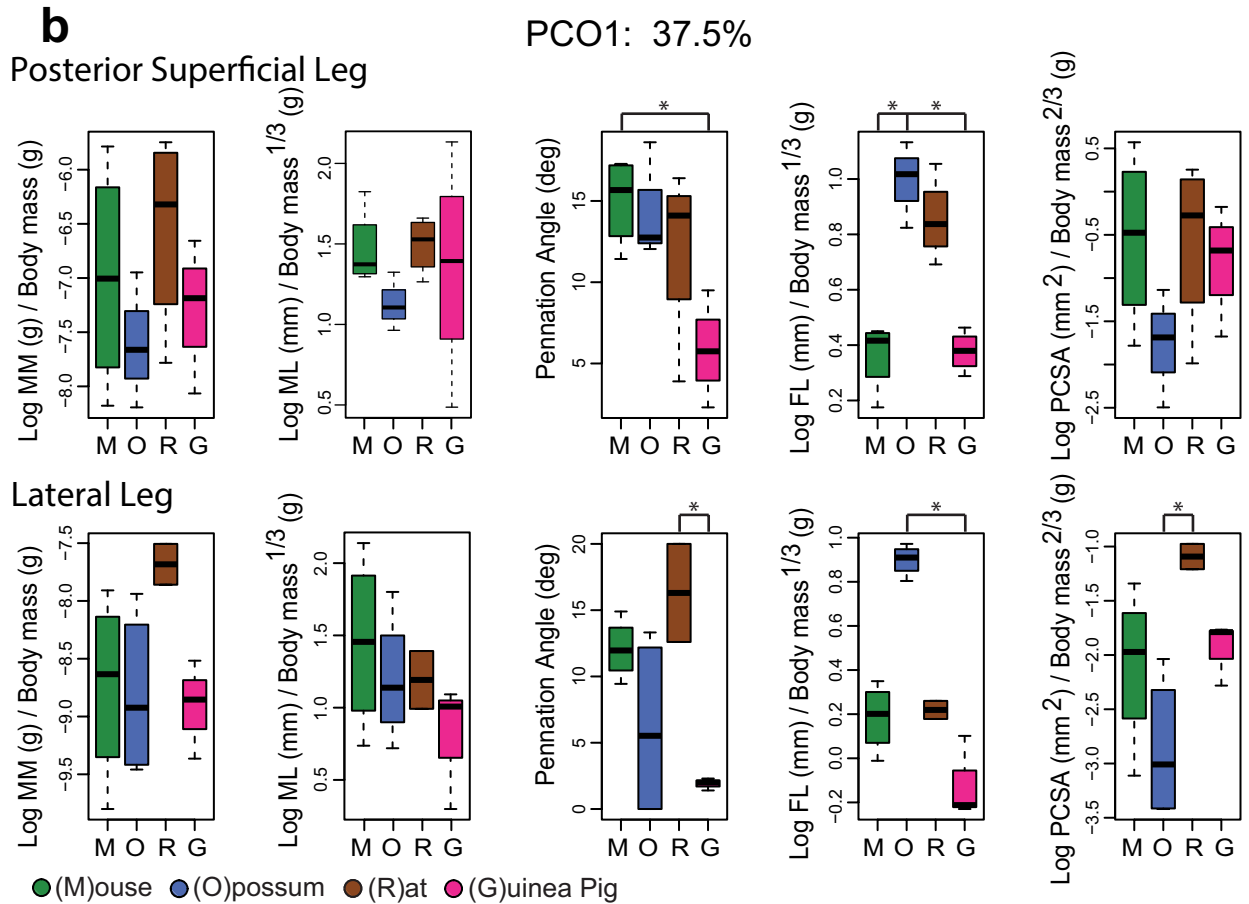
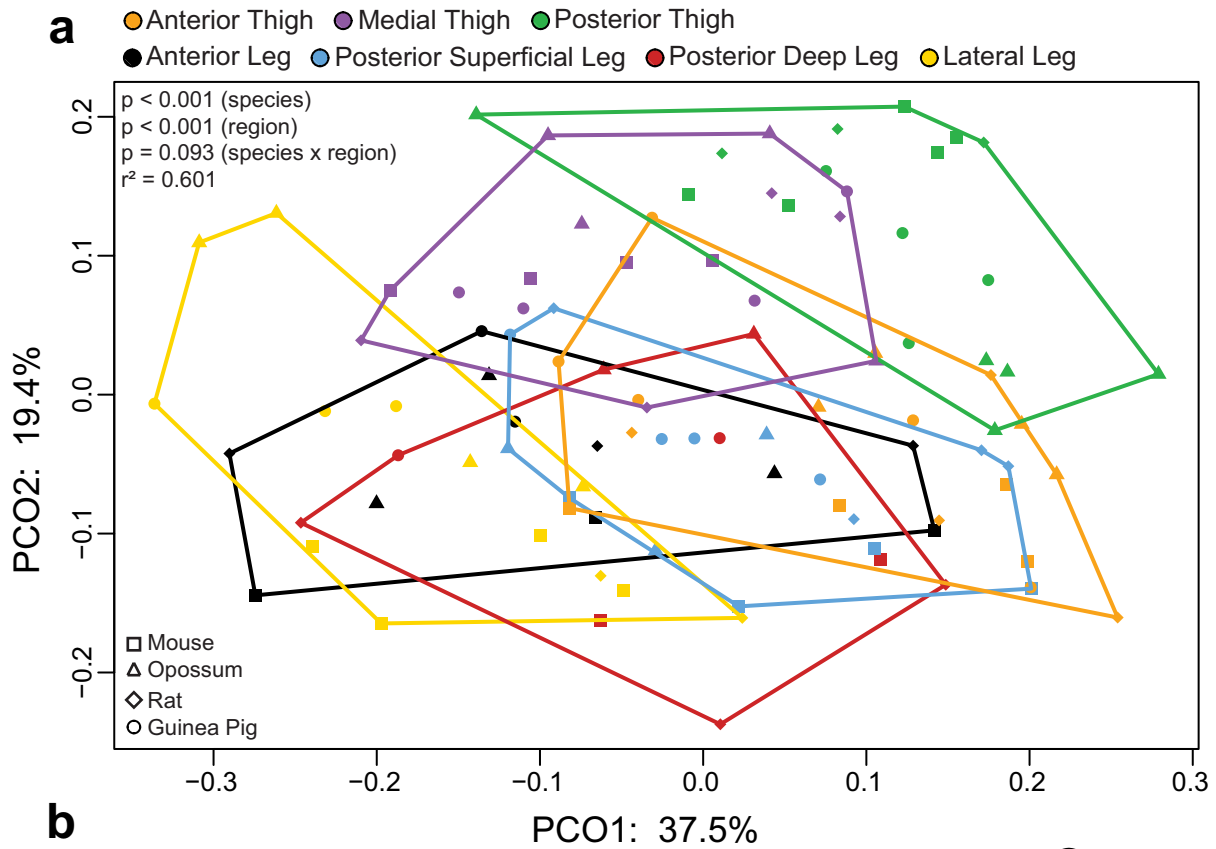


Fig. 5 a Principal coordinate analysis (PCO) of regional hindlimb muscle properties (excluding TR and PH regions) and result of non-parametric MANOVA with muscles grouped by region (indicated by color) and species (indicated by icon). **b** ANOVA results for each muscle architecture property for the two muscle regions with significant species effects: Posterior Superficial Leg and Lateral Leg. Significant pairwise species differences are indicated above each bar plot by an asterisk. Full ANOVA results can be found in Online Resource 2, Tables S4-S5

pairwise species comparisons showed that, while variation in muscle architecture exists in a few regions throughout the hindlimb, the majority of regions have indistinguishable muscle architecture.

Individual analyses of each of the nine anatomical regions identified only two regions where species significantly explained variation in muscle architecture (Online Resource 2, Table S3): Posterior Superficial Leg (PSL; $p=0.012$, $r^2=0.423$) and Lateral Leg (LL; $p=0.003$, $r^2=0.523$). For these two regions, univariate ANOVAs for each muscle property (Fig. 5b; Online Resource 2, Tables S4-5) found that the mouse had muscles with larger pennation angles than the guinea pig in the PSL ($p=0.007$). Additionally, the opossum had muscles with longer fascicles than the mouse ($p=0.004$) and the guinea pig ($p=0.005$) in the PSL, and it had muscles with longer fascicles than the guinea pig ($p<0.001$) in the LL. Finally, the rat had muscles with larger pennation angles than the guinea pig in the LL ($p=0.008$) and larger PCSAs than the opossum in the LL ($p=0.003$).

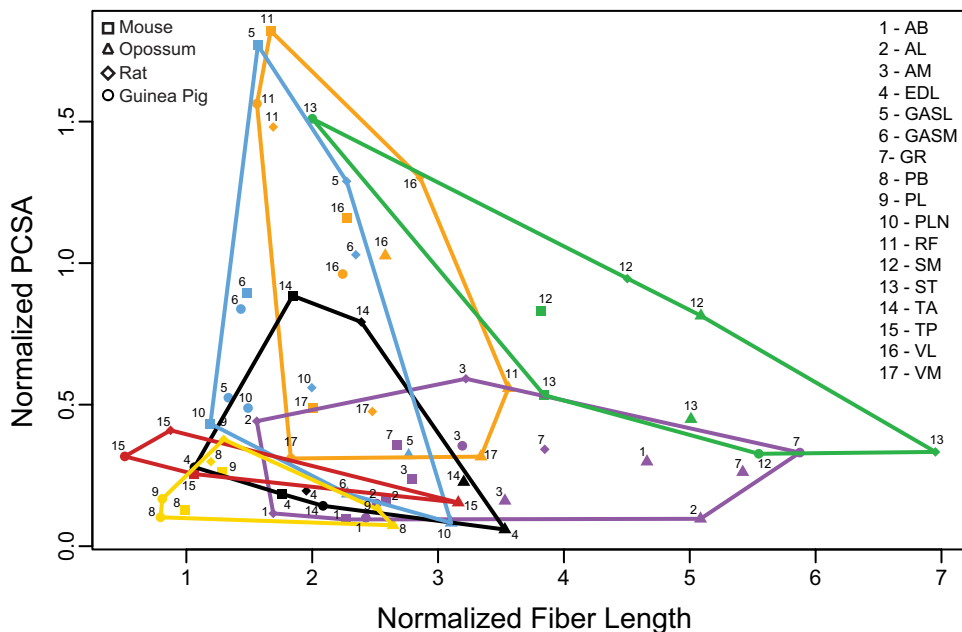
The muscles with the largest PCSA across taxa were from the Anterior Thigh (AT) and Posterior Superficial Leg (PSL) regions (Fig. 6). Specifically, the GASL, GASM, RF, and VM from these two regions had high estimated

capability for force production in the four mammals studied. The muscles with the longest fascicles across taxa were from the Medial Thigh (MT) and Posterior Thigh (PT) regions. With the exception of the ST in the guinea pig which had a large PCSA, muscles from these two regions (e.g., SM, ST, and GR) had large estimated active working ranges. In the Anterior Leg (AL) region, the TA of the mouse and rat had medium size PCSA; however, the TA in the opossum and guinea pig, as well as the EDL and all muscles in the Posterior Deep Leg (PDL) and Lateral Leg (LL) across all four species, were specialized for neither force production nor large active working ranges. These muscles typically have the bulk of their mass closer to the proximal knee joint with longer tendons extending all the way to the pes.

Discussion

Broadly, our results indicate largely indistinguishable muscle architecture properties among the hindlimbs of small-bodied, generalist mammals at both the whole limb and regional perspective (Fig. 4, 5, and 6; Online Resource 2, Tables S3-6). This finding may suggest either deep conservation of muscle architecture properties or a biomechanical constraint for hindlimb muscles in mammals of this size and ecology. Considering therians diverged at the latest by the late Middle Jurassic (Luo et al. 2011) and the musculoskeletal system is strongly influenced by allometry (Biewener 2005; Bishop et al. 2021), constraint is the more likely explanation. As a consequence, our findings may extend to small-bodied Mesozoic mammals with generalist ecological habits and morphologies. However, two caveats must be

Fig. 6 Normalized physiological cross-sectional area (PCSA) plotted against normalized fiber length (FL) for 17 homologous muscles across the four species in this study. Muscles are grouped by region (indicated by the same colors as in Fig. 5a) and species (indicated by icon). Muscles are labeled by number as indicated in legend on the right, and muscle abbreviations can be found in Table 1



acknowledged. First, the current study has a small sample size due to the limited availability of muscle architecture data in the literature for small species and challenges associated with collecting such data (including acquisition of taxonomically diverse small-bodied mammals and performing detailed dissections of very small muscles). It is possible that further sampling of other small mammal species in the future may recover more differences than identified here. Second, this study did not incorporate phylogenetic correction as no current method is able to support a data structure with large polytomies as is the case here. If phylogenetic corrections were to be applied, some instances of identified species differences in muscle architecture might instead be due to shared evolutionary histories. However, this result would only increase support for our findings. Finally, it is also important to consider forelimb musculature and test if the pattern recovered here holds beyond the hindlimb.

Whether traversing roots and plant debris on the forest floor, scurrying up and down small branches higher in the canopy, or navigating a diverse array of other terrestrial habitats, small mammals more than large mammals encounter a biomechanical challenge to maintain stable locomotion without falling and perform quick accelerations and decelerations to avoid predation (Biewener 1983; Jenkins 1987). Muscles are key for performing these behaviors. Here, we demonstrate that hindlimb muscles of small-bodied, generalist mammals show specialization according to limb region. The Anterior Thigh (AT) and Posterior Superficial Leg (PSL) regions (the latter of which contains the bulk of its muscle mass closer to the knee than the foot) produce propulsive forces at the end of stance phase and during the start of swing phase and aid in maintaining stable postures (Fischer et al. 2002; Ellis et al. 2014). These hindlimb regions included muscles with the highest normalized PCSAs across species in our dataset (Fig. 6). The Medial (MT) and Posterior Thigh (PT) regions return the femur to an approximately horizontal position during swing phase (Witte et al. 2002) and contain muscles with the longest fascicles across species in our dataset (Fig. 6). Distal leg muscles, which were neither specialized for force production nor active working ranges (and thus have low PCSAs and short fascicle) (Fig. 6), have long tendons inserting on the foot with mass distributed more closely to the trunk of the animal, which decreases resistance to limb rotation due to lowered moments of inertia (Biewener 1989, 2005; Walter and Carrier 2002). This hindlimb muscle architecture pattern, in conjunction with a morphologically similar skeletal repertoire (Sargis 2002; Álvarez et al. 2013; Chen and Wilson 2015; Hedrick et al. 2020; Weaver and Grossnickle 2020), may enable small, generalist mammals to proficiently meet the biomechanical demands associated with navigating uneven, shifting substrates, which are common among many terrestrial, scansorial, and arboreal environments. However,

mammals with highly specialized locomotor ecologies may diverge from this pattern. For instance, kangaroo rats, which are similarly small in size but are highly adapted for leaping, exhibit an increased muscle cross-sectional area (and allometric scaling exponent) throughout the hindlimb, potentially reflecting how specialization away from a generalist ecology may correspond to changes in muscle architecture (Freymler et al. 2021).

While hindlimb muscle architecture is largely indistinguishable among the species in this study, there are a few exceptions that appear among the distal regions of the limb (Fig. 5b; Online Resource 2, Tables S5 and S6). In our analysis, the most proximal (Trunk and Proximal Hip) and intermediate (Anterior, Medial, and Posterior Thigh) regions of the hindlimb had no significant pairwise species differences. However, in the most distal regions (Anterior, Posterior Superficial, Posterior Deep, and Lateral Leg), we identified six significant pairwise species differences. Of note here, we detected longer fibers in the Posterior Superficial Leg of the opossum relative to the mouse and guinea pig and in the Lateral Leg of the opossum relative to the guinea pig (Fig. 5b; Online Resource 2, Tables S4 and S5). Muscles located in these two regions presumably function to plantarflex and evert the foot (Charles et al. 2016), and longer fibers indicate the opossum can produce force across a greater active working range during these movements. While *Monodelphis domestica* is the most terrestrial member of the otherwise arboreal Didelphidae, it still retains climbing abilities and has a grasping foot morphology (Shapiro et al. 2014); therefore, longer fibers in the distal leg may represent a minor-in-degree specialization for climbing in this species. Given that proximal bony elements of the limb skeleton are more similar (Amson and Kilbourne 2019; Hedrick et al. 2020) while distal bony elements exhibit more disparity associated with locomotor specializations (Jenkins and McClearn 1984; Meldrum et al. 1997; Zeffler and Norberg 2003; Zeffler et al. 2003; Kirk et al. 2008; Samuels and Valkenburgh 2008; Chen and Wilson 2015), it may be the case that the closer a musculoskeletal structure is to the substrate with which the animal interacts, the more likely it is to reflect some kind of adaptation for interaction specifically with that substrate. Further, because distal elements of the limb form later during development, it is possible that they are more plastic and less conserved than proximal limb elements (Cooper et al. 2009; Sears et al. 2017).

Collectively, our results provide initial evidence of a common muscle architecture pattern in the hindlimb of small-bodied, generalist mammals that is proficient at meeting the biomechanical challenges associated with navigating a variety of terrestrial environments at small size. In addition, muscle architecture adaptations for specialized behaviors might increase distally throughout the limb, corresponding to more direct interactions with substrate. Future research

should especially consider pedal musculature in this regard as well as moving toward a more integrated understanding of limb mechanics among small mammals, including other properties such as muscle leverage and joint mobility (e.g., Charles et al. 2016). Beyond muscles, tendons are also a critical component of the musculoskeletal system, and while comparative tendon property data are not available for the species in this study, it is possible that differences exist and that such differences could modulate finer-scale limb function (McGuigan et al. 2009). Finally, given the small sizes and generalist ecology inferred for many Mesozoic mammals, our findings may aid researchers seeking to reconstruct and model soft tissue properties during the first 100+ million years of the clade's evolutionary history.

Supplementary Information The online version contains supplementary material available at <https://doi.org/10.1007/s10914-022-09608-6>.

Acknowledgements The study was conceived and designed by S.E.P. and M.A.W.; and K.E.S. sourced and provided the opossum cadavers upon which measurements were made. M.A.W. performed the muscle dissections, 3D muscle segmentation, and statistical analyses. The manuscript was prepared by M.A.W. and S.E.P., and all authors contributed to editing the manuscript. We thank the Pierce Lab for valuable discussion and feedback throughout the project (especially Katrina Jones, Blake Dickson, and Peter Bishop).

Funding Funding for this project was partially provided by Harvard University and the National Science Foundation grants EAR-1524523 and DEB-1754459 to S.E.P., and the National Institutes of Health grant R21OD022988-03 to K.E.S.

Data Availability All data generated or analyzed for this study are included in this published article and its supplementary information files.

Declarations

Competing Interests KES is a member of the Editorial Board of the JME but was not involved in the evaluation of this manuscript.

References

- Álvarez A, Ercoli MD, Prevosti FJ (2013) Locomotion in some small to medium-sized mammals: A geometric morphometric analysis of the penultimate lumbar vertebra, pelvis and hindlimbs. *J Zool* 116(6):356–371. <https://doi.org/10.1016/j.zool.2013.08.007>
- Amson E, Kilbourne BM (2019) Trabecular bone architecture in the stylopod epiphyses of mustelids (Mammalia, Carnivora). *R Soc Open Sci* 6(10):190938. <https://doi.org/10.1098/rsos.190938>
- Argot C (2001) Functional-adaptive anatomy of the forelimb in the didelphidae, and the paleobiology of the paleocene marsupials *Mayulestes ferox* and *Pucadelphys andinus*. *J Morph* 247(1):51–79. [https://doi.org/10.1002/1097-4687\(200101\)247:1<51::AID-JMOR1003>3.0.CO;2-#](https://doi.org/10.1002/1097-4687(200101)247:1<51::AID-JMOR1003>3.0.CO;2-#)
- Azizi E, Brainerd EL, Roberts TJ (2008) Variable gearing in pennate muscles. *PNAS* 105(5):1745–1750. <https://doi.org/10.1073/pnas.0709212105>
- Biewener AA (1983) Locomotory stresses in the limb bones of two small mammals: The ground squirrel and chipmunk. *J Exp Biol* 103:131–154
- Biewener AA (1989) Mammalian Terrestrial Locomotion and Size. *J Biosci* 39(11):776–783. <https://doi.org/10.2307/1311183>
- Biewener AA (2005) Biomechanical consequences of scaling. *J Exp Biol* 208(9):1665–1676. <https://doi.org/10.1242/jeb.01520>
- Biknevicius AR, Reilly SM, McElroy EJ, Bennett MB (2013) Symmetrical gaits and center of mass mechanics in small-bodied, primitive mammals. *J Zool* 116(1):67–74. <https://doi.org/10.1016/j.zool.2012.05.005>
- Bishop KL, Pai AK, Schmitt D (2008) Whole body mechanics of stealthy walking in cats. *PLoS One* 3(11). <https://doi.org/10.1371/journal.pone.0003808>
- Bishop PJ, Wright MA, Pierce SE (2021) Whole-limb scaling of muscle mass and force-generating capacity in amniotes. *PeerJ* 9:e12574. <https://doi.org/10.7717/peerj.12574>
- Bodine SC, Roy RR, Meadows DA, Zernicke RF, Sacks RD, Fournier M, Edgerton VR (1982) Architectural, Histochemical, and Contractile Characteristics of a Unique Biarticular Muscle: the Cat Semitendinosus. *J Neurophysiol* (48):1. <https://doi.org/10.1152/jn.1982.48.1.192>
- Bonferroni CE (1936) *Teoria Statistica Delle Classi e Calcolo Delle Probabilità*. Seeber.
- Brocklehurst N, Panciroli E, Benevento GL, Benson RBJ. (2021). Mammaliaform extinctions as a driver of the morphological radiation of Cenozoic mammals. *Curr Biol* 31:1–9. <https://doi.org/10.1016/j.cub.2021.04.044>
- Carvalho P, Diniz-Filho JAF, Bini LM (2006) Factors influencing changes in trait correlations across species after using phylogenetic independent contrasts. *Evol Ecol* 20(6):591–602. <https://doi.org/10.1007/s10682-006-9119-7>
- Charles JP, Cappellari O, Spence AJ, Hutchinson JR, Wells DJ (2016) Musculoskeletal geometry, muscle architecture and functional specialisations of the mouse hindlimb. *PLoS One* 11(4). <https://doi.org/10.1371/journal.pone.0147669>
- Chen M, Wilson GP (2015) A multivariate approach to infer locomotor modes in Mesozoic mammals. *Paleobiology* 41(2):280–312. <https://doi.org/10.1017/pab.2014.14>
- Collyer ML, Adams DC (2018) RRPP: An R package for fitting linear models to high-dimensional data using residual randomization. *Methods Ecol Evol* 9(7):1772–1779. <https://doi.org/10.1111/2041-210X.13029>
- Cooper KL, Sears KE, Uygur A, et al. (2009) Patterning and post-patterning modes of evolutionary digit loss in mammals. *Nature* 511:41–45. <https://doi.org/10.1038/nature13496>
- Cuff AR, Sparkes EL, Randau M, Pierce SE, Kitchener AC, Goswami A, Hutchinson JR (2016) The scaling of postcranial muscles in cats (Felidae) II: Hindlimb and lumbosacral muscles. *J Anat* 229(1):142–152. <https://doi.org/10.1111/joa.12474>
- Dick TJM, Clemente CJ (2016) How to build your dragon: Scaling of muscle architecture from the world's smallest to the world's largest monitor lizard. *Front Zool* 13(1):8. <https://doi.org/10.1186/s12983-016-0141-5>
- Dickson BV, Pierce SE (2018) How (and why) fins turn into limbs: Insights from anglerfish. *Earth Environ Sci Trans R Soc Edinb* 109(1-2):87–103. <https://doi.org/10.1017/S1755691018000415>
- Diogo R, Bello-Hellegouarch G, Kohlsdorf T, Esteve-Altava B, Molnar JL (2016) Comparative myology and evolution of marsupials and other vertebrates, with notes on complexity, bauplan, and “scala naturae”. *Anat Rec* 299(9):1224–1255. <https://doi.org/10.1002/ar.23390>
- Diogo R, Ziermann JM, Molnar J, Siomava N, Abdala V (2018) *Muscles of Chordates: Development, Homologies, and Evolution*. CRC Press.
- Ellis RG, Sumner BJ, Kram R (2014) Muscle contributions to propulsion and braking during walking and running: Insight from external force perturbations. *Gait Posture* 40(4):594–599. <https://doi.org/10.1016/j.gaitpost.2014.07.002>

- Eng CM, Smallwood LH, Rainiero MP, Lahey M, Ward SR, Lieber RL (2008) Scaling of muscle architecture and fiber types in the rat hindlimb. *J Exp Biol* 211(14):2336–2345. <https://doi.org/10.1242/jeb.017640>
- Fahn-Lai P, Biewener AA, Pierce SE (2020) Broad similarities in shoulder muscle architecture and organization across two amniotes: Implications for reconstructing non-mammalian synapsids. *PeerJ* 8. <https://doi.org/10.7717/peerj.8556>
- Ferner K, Zeller U, Renfree MB (2009) Lung development of monotremes: evidence for the mammalian morphotype. *Anat Rec* 292(2):190–201. <https://doi.org/10.1002/ar.20825>
- Fischer MS, Schilling N, Schmidt M, Haarhaus D, Witte H (2002) Basic limb kinematics of small therian mammals. *J Exp Biol* 205(9):1315–1338
- Freckleton RP, Harvey PH, Pagel M (2002) Phylogenetic analysis and comparative data: a test and review of evidence. *Am Nat* 160(6):712–726. <https://doi.org/10.1086/343873>
- Freymler GA, Whitford MD, Schwaner MJ, McGowan CP, Higham TE, Clark RW (2021) Comparative analysis of Dipodomys species indicates that kangaroo rat hindlimb anatomy is adapted for rapid evasive leaping. *J Anat*. <https://doi.org/10.1111/joa.13567>
- Hedrick BP, Dickson BV, Dumont ER, Pierce SE (2020) The evolutionary diversity of locomotor innovation in rodents is not linked to proximal limb morphology. *Sci Rep* 10(1):1–11. <https://doi.org/10.1038/s41598-019-57144-w>
- Jenkins FA (1971) Limb posture and locomotion in the Virginia opossum (*Didelphis marsupialis*) and in other non-cursorial mammals. *J Zool* 165(3):303–315. <https://doi.org/10.1111/j.1469-7998.1971.tb02189.x>
- Jenkins FA (1987) Tree shrew locomotion and the origins of primate arborealism. In: Ciochan RL, Fleagle JG (eds) *Primate Evolution and Human Origins*, Routledge, New York, 12 pp. <https://doi.org/10.4324/9781315127408-2>
- Jenkins FA, McClearn D (1984) Mechanisms of hind foot reversal in climbing mammals. *J Morph* 182(2):197–219. <https://doi.org/10.1002/jmor.1051820207>
- Ji Q, Luo Z-X, Yuan C-X, Tabrum AR (2006) A swimming mammaliaform from the Middle Jurassic and ecomorphological diversification of early mammals. *Science* 311(5764):1123–1127. <https://doi.org/10.1126/science.1123026>
- Jones KE, Angielczyk KD, Polly PD, Head JJ, Fernandez V, Lungmus JK, Tulga S, Pierce SE (2018) Fossils reveal the complex evolutionary history of the mammalian regionalized spine. *Science* 361(6408):1249–1252. <https://doi.org/10.1126/science.aar3126>
- Jones KE, Bielby J, Cardillo M, et al. (2009). PanTHERIA: A species-level database of life history, ecology, and geography of extant and recently extinct mammals. *Ecology*, 90(9):2648–2648. <https://doi.org/10.1890/08-1494.1>
- Kemp TS (2005) *The Origin and Evolution of Mammals*. Oxford University Press.
- Kielan-Jaworowska Z, Cifelli RL, Luo Z-X (2004) *Mammals from the Age of Dinosaurs: Origins, Evolution, and Structure*. Columbia University Press.
- Kilbourne BM (2021) Differing limb functions and their potential influence upon the diversification of the mustelid hindlimb skeleton. *Biol J Linn Soc*. <https://doi.org/10.1093/biolinnean/blaa207>
- Kirk EC, Lemelin P, Hamrick MW, Boyer DM, Bloch JI (2008) Intrinsic hand proportions of euarchontans and other mammals: Implications for the locomotor behavior of plesiadapiforms. *J Hum Evol* 55(2):278–299. <https://doi.org/10.1016/j.jhevol.2008.02.008>
- Kubo T, Sakamoto M, Meade A, Venditti C (2019) Transitions between foot postures are associated with elevated rates of body size evolution in mammals. *PNAS* 116(7):2618–2623. <https://doi.org/10.1073/pnas.1814329116>
- Lammers AR, Earls KD, Biknevicius AR (2006) Locomotor kinetics and kinematics on inclines and declines in the gray short-tailed opossum *Monodelphis domestica*. *J Exp Biol* 209(20):4154–4166. <https://doi.org/10.1242/jeb.02493>
- Lieber RL (2002) *Skeletal Muscle Structure, Function, and Plasticity*. Lippincott Williams and Wilkins.
- Luo Z-X (2007) Transformation and diversification in early mammal evolution. *Nature* 450(7172):1011–1019. <https://doi.org/10.1038/nature06277>
- Luo Z-X, Wible JR (2005) A Late Jurassic digging mammal and early mammalian diversification. *Science* 308(5718):103–107. <https://doi.org/10.1126/science.1108875>
- Luo Z-X, Yuan C-X, Meng Q-J, Ji Q (2011) A Jurassic eutherian mammal and divergence of marsupials and placentals. *Nature* 476(7361):442–445. <https://doi.org/10.1038/nature10291>
- Lyson TR, Miller IM, Bercovici AD, et al. (2019) Exceptional continental record of biotic recovery after the Cretaceous–Paleogene mass extinction. *Science*. <https://doi.org/10.1126/science.aay2268>
- McClain CR, Balk MA, Benfield MC, et al. (2015). Sizing ocean giants: Patterns of intraspecific size variation in marine megafauna. *PeerJ* 3, e715. <https://doi.org/10.7717/peerj.715>
- McGuigan MP, Yoo E, Lee DV, Biewener AA (2009) Dynamics of goat distal hind limb muscle–tendon function in response to locomotor grade. *J Exp Biol* 212(13):2092–2104. <https://doi.org/10.1242/jeb.028076>
- Meldrum DJ, Dagosto M, White J (1997) Hindlimb suspension and hind foot reversal in *Varecia variegata* and other arboreal mammals. *Am J Phys Anthropol* 103(1), 85–102.
- Meng J, Hu Y, Wang Y, Wang X, Li C (2006) A Mesozoic gliding mammal from northeastern China. *Nature* 444(7121):889–893. <https://doi.org/10.1038/nature05234>
- Nowak RM (2018) *Walker’s Mammals of the World: Monotremes, Marsupials, Afrotherians, Xenarthrans, and Sundatherians*. Johns Hopkins University Press, Baltimore, Maryland, USA.
- Panciroli E, Benson RB, Fernandez V, et al. (2022) Postcrania of *Borealestes* (Mammaliaformes, Docodonta) and the emergence of ecomorphological diversity in early mammals. *Palaeontology*. <https://doi.org/10.1111/pala.12577>
- Parchman AJ, Reilly SM, Biknevicius AR (2003) Whole-body mechanics and gaits in the gray short-tailed opossum *Monodelphis domestica*: Integrating patterns of locomotion in a semi-erect mammal. *J Exp Biol* 206(8):1379–1388. <https://doi.org/10.1242/jeb.00267>
- Pauwels E, Van Loo D, Cornillie P, Brabant L, Van Hoorebeke L (2013) An exploratory study of contrast agents for soft tissue visualization by means of high resolution X-ray computed tomography imaging. *J Microsc* 250(1):21–31. <https://doi.org/10.1111/jmi.12013>
- Polly PD (2007) Limbs in mammalian evolution. In: Hall BK (ed) *Fins into Limbs: Evolution, Development, and Transformation*. University of Chicago Press, Chicago, pp 245–268.
- Powell PL, Roy RR, Kanim P, Bello MA, Edgerton VR (1984) Predictability of skeletal muscle tension from architectural determinations in guinea pig hindlimbs. *J Appl Physiol* 57(6):1715–1721. <https://doi.org/10.1152/jappl.1984.57.6.1715>
- R Core Team (2021) R: A language and environment for statistical computing. R Foundation for Statistical Computing, Vienna. <http://www.R-project.org>. Accessed 14 Sep 2021.
- Regnault S, Fahn-Lai P, Norris RM, Pierce SE (2020) Shoulder muscle architecture in the Echidna (Monotremata: *Tachyglossus aculeatus*) indicates conserved functional properties. *J Mamm Evol*. <https://doi.org/10.1007/s10914-020-09498-6>
- Regnault S, Pierce SE (2018) Pectoral girdle and forelimb musculoskeletal function in the echidna (*Tachyglossus aculeatus*): Insights into mammalian locomotor evolution. *R Soc Open Sci* 5(11):181400. <https://doi.org/10.1098/rsos.181400>
- Reilly SM, McElroy EJ, Biknevicius AR (2007) Posture, gait and the ecological relevance of locomotor costs and energy-saving mechanisms in tetrapods. *J Zool* 110(4):271–289. <https://doi.org/10.1016/j.zool.2007.01.003>

- Revell LJ (2012) phytools: An R package for phylogenetic comparative biology (and other things). *Methods Ecol Evol* 3(2):217–223. <https://doi.org/10.1111/j.2041-210X.2011.00169.x>
- Riskin DK, Kendall CJ, Hermanson JW (2016) The crouching of the shrew: Mechanical consequences of limb posture in small mammals. *PeerJ* 4, e2131. <https://doi.org/10.7717/peerj.2131>
- Samuels JX, Valkenburgh BV (2008) Skeletal indicators of locomotor adaptations in living and extinct rodents. *J Morph* 269(11):1387–1411. <https://doi.org/10.1002/jmor.10662>
- Sargis EJ (2002) Functional morphology of the hindlimb of tupaiids (Mammalia, Scandentia) and its phylogenetic implications. *J Morph* 254(2):149–185. <https://doi.org/10.1002/jmor.10025>
- Sears K, Maier JA, Sadier A, Sorensen D, Urban DJ (2017) Timing the developmental origins of mammalian limb diversity. *Genesis*. <https://doi.org/10.1002/dvg.23079>
- Shapiro LJ, Young JW, VandeBerg JL (2014) Body size and the small branch niche: Using marsupial ontogeny to model primate locomotor evolution. *J Hum Evol* 68:14–31. <https://doi.org/10.1016/j.jhevol.2013.12.006>
- Slater GJ (2013) Phylogenetic evidence for a shift in the mode of mammalian body size evolution at the Cretaceous-Palaeogene boundary. *Methods Ecol Evol* 4(8):734–744. <https://doi.org/10.1111/2041-210X.12084>
- Stein BR (1981) Comparative limb myology of two opossums, *Didelphis* and *Chironectes*. *J Morph* 169(1):113–140. <https://doi.org/10.1002/jmor.1051690109>
- Urban DJ, Anthwal N, Luo Z-X, Maier JA, Sadier A, Tucker AS, Sears KE (2017) A new developmental mechanism for the separation of the mammalian middle ear ossicles from the jaw. *Proc Royal Soc B* 284(1848):20162416. <https://doi.org/10.1098/rspb.2016.2416>
- Walter RM, Carrier DR (2002) Scaling of rotational inertia in murine rodents and two species of lizard. *J Exp Biol* 205(14):2135–2141
- Ward SR, Lieber RL (2005) Density and hydration of fresh and fixed human skeletal muscle. *J Biomech*. <https://doi.org/10.1016/j.jbiomech.2004.10.001>
- Weaver LN, Grossnickle DM (2020) Functional diversity of small-mammal postcrania is linked to both substrate preference and body size. *Curr Zool*. <https://doi.org/10.1093/cz/zoaa057>
- Wilson DE, Mittermeier RA (2009) *Handbook of Mammals of the World, Vol. 1: Carnivores* (1st edition). Lynx Edicions.
- Wilson DE, Mittermeier RA (2011) *Handbook of the Mammals of the World, Vol. 2: Hoofed Mammals*. Lynx Edicions.
- Witte H, Biltzinger J, Hackert R, Schilling N, Schmidt M, Reich C, Fischer MS (2002) Torque patterns of the limbs of small terrestrial mammals during locomotion on flat ground. *J Exp Biol* 205(9):1339–1353
- Zeffer A, Johansson LC, Marmebro Å (2003) Functional correlation between habitat use and leg morphology in birds (Aves). *Biol J Linn Soc* 79(3):461–484. <https://doi.org/10.1046/j.1095-8312.2003.00200.x>
- Zeffer A, Norberg UML (2003) Leg morphology and locomotion in birds: Requirements for force and speed during ankle flexion. *J Exp Biol* 206(6):1085–1097. <https://doi.org/10.1242/jeb.00208>